Phosphorus stress induces the synthesis of novel glycolipids in *Pseudomonas aeruginosa* that confer protection against a last-resort antibiotic

Running title: ecophysiology of lipid renovation in Pseudomonas aeruginosa

Rebekah A. Jones[1,2], Holly Shropshire[2], Caimeng Zhao[3], Andrew Murphy[2], Ian Lidbury[2,4], Tao Wei[3], David J Scanlan[2], Yin Chen[2]

[1]MRC Doctoral Training Partnership, University of Warwick, Coventry, CV4 7AL, UK.

[2]School of Life Sciences, University of Warwick, Coventry, CV7, 7AL, UK

[3]School of Food and Biological Engineering, Zhengzhou University of Light Industry, Zhengzhou, 450002, China

[4]Department of Animal and Plant Sciences, University of Sheffield, Sheffield, S10 1AE, UK

Correspondence to Yin Chen, (email, y.chen.25@warwick.ac.uk, phone 00 44 24 76528976)

Classification: *Integrated genomics and post-genomics approaches in microbial ecology*

Abstract

Pseudomonas aeruginosa is a nosocomial pathogen with a prevalence in immunocompromised individuals and is particularly abundant in the lung microbiome of cystic fibrosis patients. A clinically important adaptation for bacterial pathogens during infection is their ability to survive and proliferate under phosphorus (P) limited growth conditions. Here, we demonstrate that *P. aeruginosa* adapts to P-limitation by substituting membrane glycerophospholipids with sugar-containing glycolipids through a lipid renovation pathway involving a phospholipase and two glycosyltransferases. Combining bacterial genetics and multi-omics (proteomics, lipidomics and metatranscriptomic analyses), we show that the surrogate glycolipids monoglycosyldiacylglycerol and glucuronic acid-diacylglycerol are synthesised through the action of a new phospholipase (PA3219) and two glycosyltransferases (PA3218 and PA0842). Comparative genomic analyses revealed that this pathway is strictly conserved in all *P. aeruginosa* strains isolated from a range of clinical and environmental settings and actively expressed in the metatranscriptome of a cystic fibrosis patient. Importantly, this phospholipid-to-glycolipid transition comes with significant ecophysiological consequence in terms of antibiotic sensitivity. Mutants defective in glycolipid synthesis survive poorly when challenged with polymyxin B, a last-resort antibiotic for treating multi-drug resistant *P. aeruginosa*. Thus, we demonstrate an intriguing link between adaptation to environmental stress (nutrient availability) and antibiotic resistance, mediated through membrane lipid renovation that is an important new facet in our understanding of the ecophysiology of this bacterium in the lung microbiome of cystic fibrosis patients.

47 **Introduction**

48 *P. aeruginosa* is a significant nosocomial pathogen in intensive care units causing
49 pneumonia, surgical wound site infections and sepsis (1-2). It is now recognised as a
50 leading cause of morbidity and mortality in chronically infected cystic fibrosis (CF) patients
51 and immunocompromised individuals due to the surge of carbapenem resistant strains, a
52 key group of first line antibiotics for treating *P. aeruginosa* infections (3). For these drug-
53 resistant *P. aeruginosa* strains, a viable but not ideal treatment option are polymyxins,
54 considered to be last resort antibiotics. Although polymyxins are active against *P.*
55 *aeruginosa*, their use was originally discontinued due to concerns over toxicity (4). Indeed,
56 *P. aeruginosa* has started to develop mechanisms of resistance to polymyxins due to
57 increase in their use globally. These primarily include modifications to the
58 lipopolysaccharide (LPS) layer of the outer membrane through the addition of 4-amino-4-
59 deoxy-L-arabinose (L-Ara4N) or phosphoethanolamine (pEtN) (5-6). These changes
60 perturb the electrostatic interaction between cationic polymyxins and normally negatively
61 charged LPS.

62

63 Glycerophospholipids, such as phosphatidylglycerol (PG) and phosphatidylethanolamine
64 (PE), are the major lipids forming the membrane lipid bilayer in bacteria, archaea and
65 eukaryotes (7-11). They play a fundamental role in the evolution of the cell and it is widely
66 accepted that the last universal common ancestor possessed a phospholipid membrane
67 (12-13). Although it is uncertain why evolution selected glycerophospholipids as the
68 building blocks for maintaining cellular membranes (13), it is known that organisms can
69 alter their membrane lipid composition in response to nutrient stress or environmental
70 changes (7, 14). Previous studies have firmly established the link between nutrient stress,
71 particularly phosphorus (P) availability, and the expression of a variety of virulence factors
72 in *P. aeruginosa* (15-19). However, it is unclear whether adaptation to P limitation in this

73 bacterium causes a change in membrane lipid composition and, if so, whether lipid
74 remodelling comes with unforeseen ecophysiological consequences. Using a synthesis of
75 multi-omics approaches, here we show that *P. aeruginosa* produces surrogate glycolipids
76 to replace phospholipids in response to P limitation. This lipid renovation pathway is strictly
77 conserved in all *P. aeruginosa* strains isolated from a range of clinical settings and actively
78 expressed in the metatranscriptome of a cystic fibrosis patient. Importantly, such a
79 phospholipid-to-glycolipid transition comes with a significant consequence in antibiotic
80 sensitivity, in that glycolipids confer protection when challenged with the antimicrobial
81 peptide polymyxin B. This work highlights more generally how the 'natural' physiological
82 adaptation of a pathogen to its *in situ* environment – in this case the P-depleted
83 environment of the human lung – can mediate a physiological response that has profound
84 implications for the survival of the bacteria in the lung microbiome.
85
86
87 **Materials and methods**
88 **Cultivation of *P. aeruginosa* and mutants**
89 *P. aeruginosa* strain PAO1 was obtained from the DSMZ culture collection (Germany) and
90 routinely cultured in lysogeny broth (LB). A defined medium previously outlined for
91 *Pseudomonas* species to control phosphate levels was also used (20). This modified
92 minimal media A comprised: Na-succinate 20 mM, NaCl 200 mg L^{-1}, NH_4Cl 450 mg L^{-1},
93 $CaCl_2$ 200 mg L^{-1}, KCl 200 mg L^{-1}, $MgCl_2$ 450 mg L^{-1}, with trace metals $FeCl_2$ 10 mg L^{-1}
94 and $MnCl_2$ 10 mg L^{-1}, with 10 mM 4-(2-hydroxyethyl)-1-piperazineethanesulfonic acid
95 (HEPES) buffer used at pH 7. Na_2HPO_4 was then added to a final concentration of 50 µM
96 (low P) or 1 mM (high P). An intermediate phosphate source of 400 µM Na_2HPO_4 was
97 used for overnight cultures in some experiments to prevent any excess storage of
98 phosphate that could hamper results. All components were filter sterilised using 0.22 µm

99 pore-size filters, and made up using double deionised H_2O. Mutants were obtained from
100 the *P. aeruginosa* strain PAO1 transposon mutant library at the University of Washington,
101 and confirmed using PCR and subsequent sequencing.
102
103 **Alkaline phosphatase assay**
104 Alkaline phosphatase activity was monitored as a measure of phosphate stress. Liquid *P.*
105 *aeruginosa* culture samples were incubated with 10 mM *para*-nitrophenol phosphate
106 (*p*NPP) to a final concentration of 1 mM. Yellow-*p*NP supernatant was measured in
107 triplicates at 407 nm (BioRad iMark microplate reader). Readings were normalised using
108 both a Tris-only incubation control and further by bacterial density (optical density reading
109 at 600 nm (OD_{600})).
110
111 **Over-expression of Agt1 and Agt2 in *E. coli***
112 *P. aeruginosa* genes PA3218 (*agt1*) and PA0842 (*agt2*) were codon optimised for *E. coli*
113 and chemically synthesised (GenScript) into plasmid pET-28a(+). *E. coli* BLR(DE3)
114 competent cells were thawed for 5 minutes before incubation with 10 ng pET-28a_Agt
115 plasmid, and placed on ice for 5 minutes. Cells were then subjected to heat shock at 42°C
116 for 30 seconds, placed back on ice for 2 minutes. Recovery SOC media was added, with
117 samples incubated at 37°C shaking, for 1 hour. Transformed cells were then plated onto
118 kanamycin-LB agar, grown overnight at 37°C. To harvest cells for lipid extraction, single
119 colonies were picked to grow in small volume LB-Kan to 0.6 OD_{600} before induction with
120 0.4 mM IPTG overnight at 25°C. 1 mL samples were then pelleted at 10,000 x *g* for 5
121 minutes. Pellets were stored at -80°C until lipid extraction and subsequent analysis on
122 HPLC-MS.
123 To purify the Agt1 and Agt2 proteins from recombinant *E. coli*, IPTG was added to
124 a final concentration of 0.5 mM once the cultures reached an OD_{600} of 0.6. After a further

125 12 h of growth at 30°C, the cells were harvested by centrifugation and resuspended in
126 buffer A containing 50 mM Tris-HCl, pH 7.9, 50 mM NaCl. Cells were disrupted by
127 sonication and 1% (w/v) of triton X-100 was then added which was then incubated for 2.5
128 hr at 4°C. The cells were then centrifuged at 12,000 × *g* for 20 min, and the soluble fraction
129 was loaded onto a nickel column (GE Healthcare, USA) pre-equilibrated with buffer A. The
130 recombinant Agt1 and Agt2 enzymes were eluted with an elution buffer (20 mM Tris-HCl,
131 pH 7.9, 500 mM NaCl, 300 mM imidazole) and dialyzed overnight into buffer A to remove
132 imidazole. For further purification, the samples were dialyzed overnight into buffer B
133 containing 50 mM Tris-HCl, pH 7.9, 200 mM NaCl, concentrated by ultrafiltration using a
134 30-kDa membrane (Millipore), and loaded onto a Superdex 200 (16/60) gel filtration
135 column (GE Healthcare, USA), which was pre-equilibrated with buffer B (50 mM Tris-HCl,
136 pH 7.9, 200 mM NaCl). The fraction size was 0.5 ml, and the flowrate was 0.5 ml/min.
137 Purified protein was analysed by SDS-PAGE, and protein concentrations were determined
138 using the Bradford assay.
139
140 **Membrane lipid extraction and HPLC-MS analysis**
141 Intact polar membrane lipids were extracted using a modified version of the typically used
142 Folch extraction method (21, 22). Liquid *P. aeruginosa* cultures growing in high and low
143 phosphate modified minimal medium A were sampled after 8 hrs, collecting the equivalent
144 to 0.5 OD_{600} into a 2 mL glass chromacol vial (Thermo Scientific), pelleted at 4°C, 4,000
145 rpm for 15 minutes. For lipid extraction, a ratio of 500:300:1000 µL of
146 methanol:water:chloroform (all LC-MS grade) was used. The lipid fraction was collected
147 from the lower phase using a glass Pasteur pipette. This chloroform extract was then dried
148 under a stream of nitrogen (Techne sample concentrator) and resuspended in 1 mL 95%
149 (v/v) acetonitrile (HPLC grade): 5% (w/v) ammonium acetate (10 mM, pH 9.2) for analysis.
150 Extracted lipid samples were analysed using an UltiMate 3000 HPLC (Thermo Scientific)

151 system coupled to AmazonSL quadrupole ion trap (Bruker) mass spectrometer (MS),
152 using electrospray ionisation. Hydrophilic interaction chromatography (HILIC) using a
153 BEH amide XP column (Waters) was utilised to separate lipid classes based on their head
154 group (35). The column chamber was maintained at 30°C and the samples passed
155 through at a 150 µL min^{-1} flow rate. The mobile phase of acetonitrile:ammonium acetate
156 (pH 9.2) was used to elute the sample in a 15 minute per sample gradient, from 95% to
157 28% ammonium acetate. The lipid d17:1/12:0 sphingosylphosphoethanolamine (Sigma-
158 Aldrich, 50 nM) was added to the samples and used as internal standard. Tandem MS (or
159 MS^n) was used to fragment the intact lipids for identification. The data were analysed using
160 Bruker Compass software package (DataAnalysis and QuantAnalysis).
161
162 **Enzyme activity assays**
163 The glycosyltransferase activity of Agt1 and Agt2 was measured using uridine
164 diphosphate (UDP)-glucose or UDP-glucuronic acid and 0.1 mM C16:0/C18:1
165 diacylglycerol (DAG) as the substrate. 2.0 µM purified enzyme was used in 10 mM
166 Tricine/KOH buffer, pH 8.5 with 2 mM dithiothreitol. The resulting mixture (500 µl) was
167 incubated at 30°C for 60 min with constant shaking at 200 rpm. The lipid products were
168 extracted using the Floch method as described above. The lipid extracts were further
169 analysed by LC-MS for the identification of MGDG/GADG though MS^n fragmentation and
170 for the quantification of DAG against standards. The K_m and V_{max} values were calculated
171 using Michaelis-Menten plots with various concentrations of UDP-sugars (0.1 to 1.0 mM)
172 in three replicates.
173
174 **Antibiotic sensitivity assays**
175 *P. aeruginosa* cultures were grown to an OD_{600} of 0.6 in high or low phosphate minimal
176 media A (see above). Cultures were then diluted 1:100 in prewarmed minimal media A

177 containing 4 µg mL^{-1} polymyxin B sulfate (Sigma). Samples were incubated at 37°C, 180
178 rpm, and assayed for survivors at specified time points by serial dilution plating onto LB.
179 *E. coli* cultures containing pET-28a-Agt1 or pET-28a-Agt2 were grown to an OD_{600} of 0.6
180 in LB broth, and the expression of Agt1 and Agt2 was induced by incubation with 0.4 mM
181 IPTG overnight at 25°C. A negative control of *E. coli* containing the pET-28a vector only
182 was also set up. Overnight cultures were diluted 1:100 in prewarmed LB broth containing
183 0.4 mM IPTG and 20 µg mL^{-1} polymyxin B sulfate (Sigma). Samples were incubated at
184 37°C, 180 rpm, and assayed for survivors at specified time points by serial dilution plating
185 onto LB agar + kanamycin 25 µg mL^{-1}.
186
187 **Comparative proteomic analysis**
188 *P. aeruginosa* PAO1 WT (1 mM phosphate, 50 µM phosphate) and PlcP mutant (50 µM
189 phosphate) cell pellets in three biological replicates were resuspended in LDS (lithium
190 dodecyl sulfate) sample buffer containing 1% β-mercaptoethanol before lysing at 95°C
191 and vortexing. 30 µL of each sample were run on NuPAGE 10% Bis-Tris protein gel
192 (Invitrogen) for a short time before staining with SafeStain (Thermo Fisher) and excising
193 the whole protein band. In-gel proteins were de-stained using 50% (v/v) ethanol, 50 mM
194 ammonium bicarbonate (ABC), before being reduced and alkylated for 5 min at 70°C using
195 10 mM TCEP (tris(2-carboxyethyl)phosphine) and 40 mM CAA (2-chloroacetamide),
196 respectively. After washing with 50% (v/v) ethanol 50 mM ABC, peptides were lysed
197 overnight using trypsin. Finally, peptides were extracted by sonication in a water bath (10
198 min at room temperature), concentrated using a Speed-Vac (50 mins) and resuspended
199 in 2.5% acetonitrile 0.05% formic acid. Extracted peptides were analysed by nanoLC-ESI-
200 MS/MS using the Ultimate 3000/Orbitrap Fusion instrumentation (Thermo Scientific). The
201 UniProt proteome for *P. aeruginosa* strain PAO1 was used for peptide analysis. Further
202 data analysis was carried out using MaxQuant and Perseus software; peptides without

203 triplicate measures were filtered out. Comparative proteomics data are presented in
204 supplementary Table S1, S3.
205
206 **Phylogenomics and metatranscriptomics analyses**
207 The protein sequences of PA3219, PA3218 and PA0842 were used to search genome
208 sequences of *Pseudomonas* clades in the JGI IMG genome portal
209 (https://img.jgi.doe.gov/). Note that the PA3218 protein is incorrectly annotated in the
210 genome of PAO1. The putative glycosyltransferase located immediately downstream of
211 PA3219 was manually inspected by aligning to the corresponding gene (PA14_22600) in
212 the genome of *P. aeruginosa* PA14. To identify PA3218 in misannotated *P. aeruginosa*
213 genomes, the nucleotide sequence immediately downstream of PA3219 was aligned with
214 PA14_22600. The phylogeny of *Pseudomonas* clades was determined using the
215 nucleotide sequences of six housekeeping genes (*rpoB, rpoD, dnaE, recA, atpD, gyrB*)
216 retrieved from each genome using IQ-Tree with the parameters -m TEST -bb 1000 -alrt
217 1000. The most suitable model was chosen by the software. Evolutionary distances were
218 inferred using maximum-likelihood analysis. Relationships were visualised using the
219 online platform the Interactive Tree of Life viewer (https://itol.embl.de/). Conserved Pho
220 box sequence was predicted using the MEME server (23).
221 The metatranscriptomics datasets of sputum samples obtained from a CF patient
222 7-days (SRX5145606) and 8-days (SRX5145605) before death (24) were retrieved from
223 the short reads archive (SRA) database (https://www.ncbi.nlm.nih.gov/sra). The reads
224 were downloaded using fastq-dump and mapped using the BBMap aligner as described
225 previously (25). Briefly, the SRA reads were mapped to the genome sequence of *P.*
226 *aeruginosa* PAO1 using a stringent cut-off of minid=0.97. Relative abundance data were
227 compared using RPKM (reads per kilobase of transcript, per million mapped reads). The

228 list of RPKM abundance of individual genes of *P. aeruginosa* PAO1 is shown in **Suppl.**
229 **Table S4**.
230
231
232 **Results and discussion**
233 ***P. aeruginosa* produces novel glycolipids in response to Pi stress**
234 To determine changes in the membrane lipidome in response to P-stress, the model *P.*
235 *aeruginosa* strain PAO1 was grown in minimal medium under high (1 mM) or low Pi (50
236 μM) conditions (**Figure 1a**). The latter condition elicited strong alkaline phosphatase
237 activity, measured through the liberation of *para*-nitrophenol (*p*NP) from *para*-nitrophenol
238 phosphate (*p*NPP) (**Figure 1b**), this being a strong indication that cells were P-stressed.
239 Analysis of membrane lipid profiles using high performance liquid chromatography
240 coupled to mass spectrometry (HPLC-MS) revealed the presence of several new lipids
241 under Pi stress conditions (**Figure 1c**). Thus, during Pi-replete growth (1 mM phosphate),
242 the lipidome is dominated by two glycerophospholipids: phosphatidylglycerol (PG, eluted
243 at 6.8 min) and phosphatidylethanolamine (PE, eluted at 12.2 min). During Pi-stress a lipid
244 species with mass to charge ratio (*m/z*) of 623 and 649 were also found, with MS
245 fragmentation resulting in a 131 *m/z* peak, a diagnostic ion for the amino-acid containing
246 ornithine lipid. This is consistent with previous reports of ornithine lipids in the *P.*
247 *aeruginosa* membrane in response to Pi stress (26-27).
248 Further to ornithine lipids, three unknown lipids eluting at 7.7 min, 8.7 min and 9.8
249 min, were only present under Pi stress conditions (**Figure 1c**). Using several rounds of
250 MS fragmentation (MS^n), with a quadrupole ion trap MS, fragmentation patterns
251 characteristic of glycolipids were found for all three peaks. For each peak of interest, the
252 most predominant lipid masses of 774 *m/z*, 786 *m/z* and 788 *m/z* were analysed by MS^n
253 in positive ionisation mode (**Figure 1d**). In each case, an initial head group was lost

254 leaving a significant signal of 595 *m/z*, the mass of the glycolipid building block
255 diacylglycerol (DAG). Further fragmentation leads to the loss of either fatty acyl chain from
256 DAG, leaving monoacylglycerols of 313 *m/z* and 339 *m/z*. Two monoacylglycerols with
257 different masses are produced as a result of the original lipid containing 16:0 and 18:1
258 fatty acids (313 *m/z* and 339 *m/z* monoacylglycerols, respectively). To further elucidate
259 the identity of the peaks, a search for a neutral loss of a polar head group was carried out.
260 Thus, the intact masses of 774 *m/z* and 788 *m/z* in positive ionisation mode leads to the
261 loss of a head group of -179 and -193 *m/z*, which corresponds to a hexose- and a
262 glucuronate- group, respectively (**Figure 1d**), suggesting the occurrence of novel
263 monoglycosyldiacylglycerol (MGDG) and glucuronic acid diacylglycerol (GADG)
264 glycolipids in *P. aeruginosa*. The third glycolipid peak at 8.7 min remains an unknown lipid
265 with intact mass of 767 *m/z* (hereafter designated as a putative unknown glycolipid, UGL).
266 Together, these data confirm the production of new glycolipids in *P. aeruginosa* in
267 response to Pi stress.
268
269 **Comparative proteomics uncover the lipid renovation pathway in *P. aeruginosa***
270 To determine the proteomic response of *P. aeruginosa* to P limitation, and identify the
271 genes involved in glycolipid formation, strain PAO1 was cultivated under high and low Pi
272 conditions for 8 hours and the cellular proteome then analysed. A total of 2844 proteins
273 were detected using nanoLC-ESI-MS/MS instrumentation, 175 of which were found to be
274 differentially regulated by Pi availability when significance was considered at a false
275 detection rate (FDR) of <0.05 (**Figure 2b, Suppl. Table S1**). Of these, 132 proteins were
276 more highly expressed during Pi-deplete conditions, and 43 were more highly expressed
277 during Pi-replete growth conditions. In line with previous transcriptomic studies of *P.*
278 *aeruginosa* PAO1 (18), major P acquisition mechanisms were more highly expressed
279 under Pi stress conditions. These included the high-affinity Pi-specific transporter

280 PstSCAB, the two-component master regulator of the PHO regulon PhoBR, phosphate-
281 specific porins (OprO, OprP), alkaline phosphatases, phosphonate transporters,
282 extracellular DNA degradation enzymes (EddB and EddA), and a number of key virulence
283 factors (e.g. PlcH, PlcN, PlcB, **Suppl. Table S1**) (28-30).

284 Comparative proteomics also identified several genes which are likely important
285 for membrane lipid remodelling (**Figure 2a**) including PA3219 (4.6-fold increase under Pi-
286 deplete conditions, FDR<0.01), encoding a putative phospholipase C protein, and PA0842
287 (4-fold increase under Pi-deplete conditions, FDR<0.01), encoding a putative
288 glycosyltransferase (**Figure 2b**). PA3219 has 47% protein sequence identity to PlcP from
289 *Phaeobacter* sp. MED193 and 46% identity to PlcP from *Sinorhizobium meliloti* (25-27).
290 In these bacteria, PlcP is essential in the lipid remodelling pathway for the formation of the
291 diacylglycerol (DAG) backbone, representing the essential intermediate for the production
292 of glycolipids (31-32). In *P. aeruginosa* PAO1, PA3219 appears to form an operon with
293 PA3218, a putative glycosyltransferase likely under the control of the PhoBR two
294 component system, as a highly conserved Pho box sequence was recognisable in the
295 promoter region (**Figure 2c**). PA3218 (hereafter referred to as Agt1) has 41% protein
296 sequence identity to the Agt of *Phaeobacter* sp. MED193. PA0842 showed 35% identity
297 to the Agt of *Phaeobacter* sp. MED193 and a Pho box sequence is also found in its
298 promoter region. This corroborates the finding that the PA0842 protein (hereafter referred
299 to as Agt2) was significantly upregulated under Pi-deplete conditions (**Figure 2b**). In
300 summary, comparative proteomic analysis suggests that *P. aeruginosa* PAO1 adopts this
301 PlcP-Agt lipid remodelling pathway for the production of glycolipids in response to Pi-
302 stress (**Figure 2a**).
303

304 **The PlcP-Agt mediated lipid renovation pathway is strictly conserved in *P.***
305 ***aeruginosa* and actively transcribed in the metatranscriptomes of a cystic fibrosis**
306 **patient**
307 To uncover how widespread this predicted PlcP-Agt lipid remodelling pathway is amongst
308 the genus *Pseudomonas,* including *P. aeruginosa* strains, we conducted a thorough
309 comparative genomics analysis of these lipid renovating loci. PlcP-Agt is strictly conserved
310 in all 770 genome-sequenced *P. aeruginosa* strains in the IMG/M database, including all
311 three-previously recognised *P. aeruginosa* lineages (33-34), group 1 represented by strain
312 PAO1, group 2 represented by strain PA14 and group 3 represented by strain PA7 (**Figure**
313 **3, Suppl. Table S2**). Indeed, this remodelling pathway is prevalent in many *Pseudomonas*
314 groups, including the plant pathogen *Pseudomonas syringae*. To investigate whether the
315 PlcP-Agt lipid remodelling pathway is involved in host-pathogen interactions, we analysed
316 metatranscriptomic datasets from a cystic fibrosis patient, where *P. aeruginosa* is known
317 to be prevalent in the fatal exacerbation period before patient death (24). To the best of
318 our knowledge, only one study has reported the metatranscriptome of the bacterial
319 community present in CF sputum (24). Indeed, *phoBR* and *pstS* are amongst the most
320 highly expressed genes, confirming previous observations that *P. aeruginosa* is Pi-limited
321 during lung infection (1-2). Importantly, the transcripts of *P. aeruginosa agt1/plcP/agt2* are
322 also highly expressed in CF sputum during the fatal exacerbation period before death
323 (**Figure 2d**). Therefore, our phylogenomic and metatranscriptomic analyses suggest that
324 not only is the PlcP-Agt lipid remodelling pathway strictly conserved and prevalent in *P.*
325 *aeruginosa*, the genes are also highly expressed during CF patient infection, suggesting
326 a potential role for lipid renovation in host-pathogen interactions.
327
328 **Experimental validation of the lipid renovation pathway for glycolipid formation in**
329 ***P. aeruginosa***

330 To validate the function of these two putative glycosyltransferases (Agt1, Agt2) in the
331 formation of glycolipids, we synthesized the codon-optimized genes (PA3218 and
332 PA0842, respectively) for recombinant expression in *Escherichia coli*. The total lipidomes
333 from the recombinant *E. coli* strains were then analysed by HPLC-MS to determine the
334 presence of glycolipids in a gain-of-function assay. Expression of *P. aeruginosa* Agt1
335 (PA3218) was sufficient for the production of MGDG (eluted at 7.7 min) in *E. coli*,
336 confirmed through MS^n fragmentation (**Figure 4a**). No UGL nor GADG was observed in
337 the lipidome of this Agt1-overexpressing *E. coli* strain. Expressing Agt2 (PA0842) from *P.*
338 *aeruginosa* in *E. coli* was sufficient for the accumulation of the GADG glycolipid (eluted at
339 9.8 min), also confirmed through the MS^n fragmentation pattern (**Figure 4b**). Equally, no
340 UGL nor MGDG was observed in the Agt2-overexpressing *E. coli* strain. Production of
341 these glycolipids was not observed in the same strain of *E. coli* transformed with an empty
342 vector control (pET28a).

343 To confirm the role of Agt1 and Agt2 in the production of MGDG and GADG, we
344 purified Agt1 and Agt2 from recombinant *E. coli* (**Figure 4c**) and carried out enzyme
345 assays using UDP-glucose and UDP-glucuronic acid as the sugar donor and DAG as the
346 acceptor. Agt1 can only accept UDP-glucose as the substrate with an affinity of K_m=298.1
347 ± 9.5 μM (**Figure 4c**, middle panel) and produced MGDG as expected (**Figure 4d**, left
348 panel). Similarly, Agt2 can use UDP-glucuronic acid as the substrate (K_m= 373.0 ± 12.9
349 μM (**Figure 4c**, right panel), producing GADG lipid (**Figure 4d**, right panel). Interestingly,
350 the purified Agt2 enzyme can also use UDP-glucose to some extent with a K_m of 480 μM
351 (data not shown) although the corresponding lipid MGDG was not observed in the lipid
352 extract from the lipidome of the recombinant host *E. coli* (**Figure 4b**).

353 To further confirm the role of these genes in *P. aeruginosa* glycolipid biosynthesis
354 we analysed the lipidomes of mutants in *ΔplcP*, *Δagt1* and *Δagt2* in strain PAO1 (**Figure**
355 **5a, b**). Differences were analysed by searching for the intact masses of the glycolipids

356 MGDG and GADG: 774 *m/z* and 788 *m/z* in positive ionisation mode with an ammonium
357 adduct, respectively. As expected, under Pi stress MGDG is no longer produced in the
358 *Δagt1* mutant and similarly GADG is no longer produced in the *Δagt2* mutant (**Figure 5a**).
359 In the *ΔplcP* mutant, no MGDG was found and the GADG lipid was significantly reduced
360 but not entirely abolished (**Figure 5b**). The small amount of GADG produced in the *ΔplcP*
361 mutant suggests that an alternative supply of DAG (independent of the degradation of
362 phospholipids by PlcP) is available in this mutant. Nevertheless, lipidome analyses of the
363 *ΔplcP*, *Δagt1* and *Δagt2* mutants strongly supports the key role of this PlcP-Agt pathway
364 (**Figure 2A**) in lipid renovation in *P. aeruginosa*.
365

366 **The protective role of glycolipids to antibiotic resistance in *Pseudomonas***
367 ***aeruginosa***

368 The presence of glycolipids in the membrane is likely to have a profound impact on the
369 functioning of the *P. aeruginosa* membrane during Pi stress. For example, PG is an
370 anionic lipid with net negative charges whereas MGDG has a neutral charged sugar
371 group. Although a PG-to-GADG substitution may not necessarily change membrane
372 charge (36), it may affect membrane curvature and the packing density of lipids. Thus,
373 subsequent knock-on effects in membrane function might be expected (10). We therefore
374 set out to investigate whether membrane lipid composition may have an impact on
375 antibiotic resistance in *P. aeruginosa*. As cationic antimicrobial peptides directly interact
376 with bacterial cell membranes, we focused on the impact of lipid remodelling on the killing
377 activity of polymyxin B. We conducted the analyses under P-deplete conditions, since Pi-
378 stress is clinically important, already known to induce the expression of virulence factors
379 (15, 17, 18, 29), and our own analysis confirmed that *P. aeruginosa* is indeed P stressed
380 during CF lung colonisation (**Figure 2d**). Polymyxins represent the drug-of-last resort for
381 effectively treating carbapenem-resistant *P. aeruginosa* infections (3, 37).

382 To test the sensitivity of the mutants in the PlcP-Agt pathway to polymyxin B, we
383 compared WT and mutants using kill curve analyses as the typically used disk diffusion
384 method does not work efficiently for cationic antimicrobials (38). Indeed, there was a
385 significant decrease in the survival of all three PAO1 glycolipid synthesis mutants (*ΔplcP*,
386 *Δagt1* and *Δagt2*) compared to the wild type when challenged with polymyxin B,
387 suggesting a protective role of glycolipids in polymyxin B resistance (**Figure 5c**). *P.*
388 *aeruginosa* is known to enhance its resistance to polymyxins through decoration of its
389 lipopolysaccharide (LPS) layer using either 4-amino-4-deoxy-L-arabinose (L-Ara4N) by
390 *arnB* (5), or the addition of phosphoethanolamine (pEtN) by *eptA* (6). It is thought that
391 these changes perturb the electrostatic interaction between the cationic polymyxin B and
392 the normally negatively charged LPS. To investigate whether these mechanisms play a
393 role in the glycolipid-deficient mutants, we conducted a comparative proteomics analysis
394 of the *ΔplcP* mutant and WT under P deplete conditions, which revealed only a small
395 number of differentially expressed proteins (**Suppl. Table S3**). The majority of these
396 differentially expressed proteins are uncharacterised. However, importantly, LPS
397 modification enzymes previously found to confer antimicrobial peptide resistance, such as
398 ArnB and EptA, were not differentially expressed between the WT and *ΔplcP* mutant.
399 Therefore, the data suggests that these glycolipids are likely a major contributor to
400 increased polymyxin B resistance, which constitutes a new biological mechanism for
401 polymyxin resistance. To this end, we tested the resistance to polymyxin B of recombinant
402 *E. coli* strains overexpressing *P. aeruginosa* Agt1 and Agt2, that produce MGDG and
403 GADG, respectively (**Figure 4a, 4b**). Indeed, in this gain-of-function assay, both Agt1 and
404 Agt2 overexpressing *E. coli* strains had enhanced resistance to polymyxin B compared to
405 the empty vector control (**Figure 5d**), supporting the protective role of these glycolipids to
406 antimicrobial peptides.
407

408 To conclude, we present here the discovery of novel glycolipids produced in *P.*
409 *aeruginosa* during adaption to P stress in the lung microbiome. This lipid renovation
410 pathway is strictly conserved in all *P. aeruginosa* isolates to date and highly expressed in
411 the metatranscriptome of CF patients, suggesting a key role of lipid remodelling in the
412 ecophysiology of this bacterium. Interestingly, lipid remodelling as a response to survive
413 phosphorus stress in turn comes with trade-offs in terms of antibiotic resistance; the
414 glycolipids may protect the bacterium from insult by cationic antimicrobial peptides. It
415 remains to be seen whether the altered susceptibility to polymyxin B is the sole trade-off
416 following lipid remodelling of phospholipids to glycolipids. After all, evolution appears to
417 have selected phospholipids as the dominant lipids in the last universal common ancestor
418 (12).
419
420
421 **Acknowledgements**
422 This work was funded by an MRC Doctoral Training Partnership studentship in
423 Interdisciplinary Biomedical Research (MR/J003964/1) awarded to RAJ and the Royal
424 Society International Exchanges 2017 Cost Share (China) award (IEC\NSFC\170213; grant
425 agreement no. 170213). We thank the Proteomics Research Technology Platform,
426 University of Warwick, UK for their contribution.
427
428 **Competing interest**
429 The authors declare no competing interests.

430 **References**

431 **1.** Murray, T. S., Egan, M., & Kazmierczak, B. I. (2007). *Pseudomonas aeruginosa*
432 chronic colonization in cystic fibrosis patients. *Current Opinion in Pediatrics,* 19:
433 83-88.

434 **2.** Gaynes, R., Edwards, J. R., & System, N. N. I. S. (2005). Overview of nosocomial
435 infections caused by Gram-negative bacilli. *Clinical Infectious Diseases*, 41:848–
436 854.

437 **3.** Hawkey PM, Livermore DM (2012). Carbapenem antibiotics for serious infections.
438 *BMJ*. 344:e3236.

439 **4.** Landman, D., Georgescu, C., Martin, D. A., & Quale, J. (2008). Polymyxins
440 revisited. *Clinical Microbiology Reviews*. 21:449–465.

441 **5.** Chung, E. S., Lee, J. Y., Rhee, J. Y., & Ko, K. S. (2017). Colistin resistance in
442 *Pseudomonas aeruginosa* that is not linked to *arnB*. *Journal of Medical*
443 *Microbiology*, 66:833–841.

444 **6.** Nowicki, E. M., O'Brien, J. P., Brodbelt, J. S., & Trent, M. S. (2015). Extracellular
445 zinc induces phosphoethanolamine addition to *Pseudomonas aeruginosa* lipid A
446 via the ColRS two-component system. *Mol. Microbiol. 97*:166–178.

447 **7.** Parsons JB, Rock CO. (2013) Bacterial lipids: metabolism and membrane
448 homeostasis. *Prog Lipid Res.* 52:249-276.

449 **8.** Zhang, Y.-M., & Rock, C. O. (2008). Membrane lipid homeostasis in bacteria.
450 *Nature Rev. Microbiol.* 6:222–233.

451 **9.** van Meer G, Voelker DR, Feigenson GW. (2008) Membrane lipids: where they are
452 and how they behave. *Nat Rev Mol Cell Biol.* 9:112-124.

453 **10.** Harayama T, Riezman H. (2018) Understanding the diversity of membrane lipid
454 composition. *Nat Rev Mol Cell Biol.* 19:281-296.

455 **11.** May, K.L., & Silhavy T.J. (2017) Making a membrane on the other side of the wall.
456 *Biochimica et Biophysica Acta*. 1862:1386-1393.

457 **12.** Lombard J, López-García P, Moreira D. (2012) The early evolution of lipid
458 membranes and the three domains of life. *Nat Rev Microbiol.* 10:507-515.

459 **13.** Peretó J, López-García P, Moreira D. (2004) Ancestral lipid biosynthesis and early
460 membrane evolution. *Trends Biochem Sci*. 29:469-477.

461 **14.** Sahonero-Canavesi DX, López-Lara IM, Geiger O (2019) Membrane lipid
462 degradation and lipid cycles in microbes. In *Aerobic Utilization of Hydrocarbons,*
463 *Oils, and Lipids*, 10.1007/978-3-319-50418-6_38

464 **15.** Lamarche MG, Wanner BL, Crépin S, Harel J. (2008) The phosphate regulon and

465 bacterial virulence: a regulatory network connecting phosphate homeostasis and
466 pathogenesis. *FEMS Microbiol. Rev.* 32:461-473.
467 **16.** Long, J., Zaborina, O., Holbrook, C., Zaborin, A., & Alverdy, J. (2008). Depletion of
468 intestinal phosphate after operative injury activates the virulence of *P. aeruginosa*
469 causing lethal gut-derived sepsis. *Surgery*, *144*:189–197.
470 **17.** Francis VI, Stevenson EC, Porter SL. (2017) Two-component systems required for
471 virulence in *Pseudomonas aeruginosa. FEMS Microbiol Lett.* 364(11). doi:
472 10.1093/femsle/fnx104.
473 **18.** Bains, M., Fernández, L., & Hancock, R. E. W. (2012). Phosphate starvation
474 promotes swarming motility and cytotoxicity of *Pseudomonas aeruginosa*. *Applied*
475 *and Environmental Microbiology*, *78*:6762–6768.
476 **19.** Son, M. S., Matthews, W. J., Kang, Y., Nguyen, D. T., & Hoang, T. T. (2007). *In*
477 *vivo* evidence of *Pseudomonas aeruginosa* nutrient acquisition and pathogenesis
478 in the lungs of cystic fibrosis patients. *Infection and Immunity* 75:5313–5324.
479 **20.** Lidbury, I. D. E. A., Murphy, A. R. J., Scanlan, D. J., Bending, G. D., Jones, A. M.
480 E., Moore, J. D., et al., (2016). Comparative genomic, proteomic and exoproteomic
481 analyses of three *Pseudomonas* strains reveals novel insights into the phosphorus
482 scavenging capabilities of soil bacteria. *Environ. Microbiol.* 18:3535–3549.
483 **21.** Sebastián, M., Smith, A. F., González, J. M., Fredricks, H. F., Van Mooy, B.,
484 Koblížek, M., et al., (2016). Lipid remodelling is a widespread strategy in marine
485 heterotrophic bacteria upon phosphorus deficiency. *ISME J.* 10:968–978.
486 **22.** Smith AF, Rihtman B, Stirrup R, Silvano E, Mausz MA, Scanlan DJ, Chen Y. (2019)
487 Elucidation of glutamine lipid biosynthesis in marine bacteria reveals its importance
488 under phosphorus deplete growth in *Rhodobacteraceae. ISME J.* 13:39-49.
489 **23.** Bailey TL, Elkan C (1994) Fitting a mixture model by expectation maximization to
490 discover motifs in biopolymers. *Proceedings of the Second International*
491 *Conference on Intelligent Systems for Molecular Biology*, 28-36, AAAI Press,
492 Menlo Park, Californias.
493 **24.** Cobián Güemes AG, Lim YW, Quinn RA, Conrad DJ, Benler S, Maughan H,
494 Edwards R, et al. (2019) Cystic fibrosis rapid response: translating multi-omics data
495 into clinically relevant information. *mBio.* 16;10(2):e00431-19.
496 **25.** Jones, H.J., Krober, E., Stephenson, J., Mausz M.A., Jameson, E., Millard, A.,
497 Purdy, K.J., Chen, Y. (2019) A new family of uncultivated bacteria involved in
498 methanogenesis from the ubiquitous osmolyte glycine betaine in coastal saltmarsh
499 sediments. *Microbiome*. 7, 120. doi.org/10.1186/s40168-019-0732-4

500 **26.** Kim, S. K., Park, S. J., Li, X. H., Choi, Y. S., Im, D. S., & Lee, J. H. (2018). Bacterial
501 ornithine lipid, a surrogate membrane lipid under phosphate-limiting conditions,
502 plays important roles in bacterial persistence and interaction with host. *Environ.*
503 *Microbiol. 20*:3992–4008.
504 **27.** Lewenza, S., Falsafi, R., Bains, M., Rohs, P., Stupak, J., Sprott, G. D., & Hancock,
505 R. E. W. (2011). The *olsA* gene mediates the synthesis of an ornithine lipid in
506 *Pseudomonas aeruginosa* during growth under phosphate-limiting conditions, but
507 is not involved in antimicrobial peptide susceptibility. *FEMS Microbiol. Lett.* 320:
508 95–102.
509 **28.** Kida Y, Shimizu T, Kuwano K. (2011) Cooperation between LepA and PlcH
510 contributes to the in vivo virulence and growth of *Pseudomonas aeruginosa* in
511 mice. *Infect Immun.* 79:211-219.
512 **29.** Haghi F, Zeighami H, Monazami A, Toutouchi F, Nazaralian S, Naderi G. (2018)
513 Diversity of virulence genes in multidrug resistant *Pseudomonas aeruginosa*
514 isolated from burn wound infections. *Microb Pathog.* 115:251-256.
515 **30.** Wilton M, Halverson TW, Charron-Mazenod L, Parkins MD, Lewnza S. (2018)
516 Secreted phosphatase and deoxyribonuclease are required by *Pseudomonas*
517 *aeruginosa* to defend against neutrophil extracellular traps. *Infec Immun*
518 86:e00403-18.
519 **31.** Wei, T., Quareshy, M., Zhang, Y. Z., Scanlan, D. J., & Chen, Y. (2018). Manganese
520 is essential for PlcP metallophosphoesterase activity involved in lipid remodeling
521 in abundant marine heterotrophic bacteria. *Appl. Environ. Microbiol. 84,* e01109-
522 18.
523 **32.** Zavaleta-Pastor, M., Sohlenkamp, C., Gao, J.-L., Guan, Z., Zaheer, R., Finan, T.
524 M., et al., (2010). *Sinorhizobium meliloti* phospholipase C required for lipid
525 remodeling during phosphorus limitation. *Proc. Nat. Acad. Sci. USA107*:302–307.
526 **33.** Freschi L, Jeukens J, Kukavica-Ibrulj I, Boyle B, Dupont MJ, Laroche J, et al.,
527 (2015) Clinical utilization of genomics data produced by the international
528 *Pseudomonas aeruginosa* consortium. *Front Microbiol.* 29;6:1036. doi:
529 10.3389/fmicb.2015.01036.
530 **34.** Ozer EA, Nnah E, Didelot X, Whitaker RJ, Hauser AR. (2019) The population
531 structure of *Pseudomonas aeruginosa* is characterized by genetic isolation of
532 *exoU*+ and *exoS*+ lineages. *Genome Biol Evol.* 11:1780-1796.
533 **35.** Diercks H, Semeniuk A, Gisch N, Moll H, Duda KA, Hölzl G. (2015) Accumulation
534 of novel glycolipids and ornithine lipids in *Mesorhizobium loti* under phosphate

535 deprivation. *J Bacteriol.* 197:497-509.
536 **36.** Poirel L, Jayol A, Nordmann P. (2017) Polymyxins: antibacterial activity,
537 susceptibility testing, and resistance mechanisms encoded by plasmids or
538 chromosomes. *Clin Microbiol Rev*. 30:557-596.
539 **37.** Ezadi, F., Ardebili A., Mirnead R (2019) Antimicrobial susceptibility testing for
540 polymyxins: challenges, issues, and recommendations. *J. Clin. Microbiol. 57,*
541 e01390-18.
542 **38.** Monds RD, Newell PD, Schwartzman JA, O'Toole GA. (2006) Conservation of the
543 Pho regulon in *Pseudomonas fluorescens* Pf0-1. *Appl Environ Microbiol*. 72:1910-
544 1924.
545 **39.** Semeniuk A, Sohlenkamp C, Duda K, Hölzl G. (2014) A bifunctional
546 glycosyltransferase from *Agrobacterium tumefaciens* synthesizes monoglucosyl
547 and glucuronosyl diacylglycerol under phosphate deprivation. *J Biol Chem.*
548 289(14):10104-14.
549 **40.** Minh BQ, Schmidt HA, Chernomor O, Schrempf D, Woodhams MD, von
550 Haeseler A, et al. (2020) IQ-TREE 2: New models and efficient methods for
551 phylogenetic inference in the genomic era. *Mol Biol Evol*. 37:1530–1534.
552

553 **Figure legends**

554 **Figure 1 Lipidomics analysis uncovers novel glycolipid formation in *Pseudomonas***
555 ***aeruginosa* strain PAO1 in response to phosphorus limitation.**

556 **a)** Growth of strain PAO1 WT in minimal medium A containing 1 mM phosphate (+P, blue)
557 or 50 µM phosphate (-P, black) over 12 hours. Data are the average of 3 independent
558 replicates.

559 **b)** Liberation of *para*-nitrophenol (*p*NP) from *para*-nitrophenol phosphate (*p*NPP) through
560 alkaline phosphatase activity, under P-replete (1 mM, black) and P-deplete (50 µM,
561 yellow) conditions. Error bars represent the standard deviation of three independent
562 replicates.

563 **c)** Representative chromatograms in negative ionisation mode of the *P. aeruginosa*
564 lipidome when grown under phosphorus stress (-P, black) compared to growth under
565 phosphorus sufficient conditions (+P, orange). PG, phosphatidylglycerol; PE,
566 phosphatidylethanolamine, OL, ornithine lipids. Lower panel: extracted ion
567 chromatograms of three new glycolipid species in *P. aeruginosa* which are only produced
568 in P-limitation (black, 1 mM; orange, 50 µM). MGDG: monoglycosyldiacylglycerol, GADG:
569 glucuronic acid-diacylglycerol and UGL: unconfirmed glycolipid.

570 **d)** Mass spectrometry fragmentation spectra of three glycolipid species present under
571 phosphorus stress in *P. aeruginosa*, at retention times of 7.7 (*m/z* 774.7), 8.7 (*m/z* 786.7)
572 and 9.8 (*m/z* 788.6) minutes, respectively. Each spectrum depicts an intact lipid mass with
573 an ammonium (NH_4^+) adduct exhibiting neutral loss of a head group, yielding
574 diacylglycerol (DAG) (595 *m/z*). Further fragmentation yields monoacylglycerols (MAG)
575 with C16:0 or C18:1 fatty acyl chains.

576

577 **Figure 2 Comparative multi-omic analyses for the identification of the PlcP-Agt**
578 **pathway responsible for glycolipid formation in *Pseudomonas aeruginosa* strain**
579 **PAO1.**

580 **a)** The proposed pathway for lipid remodelling through the PlcP-Agt pathway. PlcP
581 degrades membrane phospholipids such as PG, to generate diacylglycerol (DAG)
582 intermediates for the formation of MGDG and GADG through the activity of
583 glycosyltransferases, using either UDP-glucose or UDP-glucuronate as the co-substrate
584 (39).

585 **b)** Volcano plot depicting differentially expressed proteins when comparing Pi-replete and
586 Pi-deplete conditions. Significantly upregulated proteins when under Pi stress are shown
587 in red (left), and those that are significantly upregulated when Pi is sufficient are in green
588 (right). Significance was accepted when the false discovery rate (FDR) was < 0.05, and a
589 fold change ≥ 2.

590 **c)** Genomic organisation of predicted lipid remodelling genes in *P. aeruginosa*.
591 Glycosyltransferases (orange) PA3218 (Agt1) and PA0842 (Agt2) are predicted to be
592 involved in glycolipid synthesis. PA3219 is predicted to be PlcP in *P. aeruginosa*.
593 Predicted Pho box sequences in the promoter regions (represented in blue boxes) of each
594 glycosyltransferase operon from *P. aeruginosa* strains representing the PAO1 clade, the
595 PA7 clade and the PA14 clade are shown. The black dots represent residues which are
596 conserved in the Pho box consensus CTGTCATNNNNCTGTCAT (38).

597 **d)** Metatranscriptomic analysis of PlcP-Agt lipid remodelling genes in sputum samples
598 from a cystic fibrosis patient 7-days (D-7) and 8-days (D-8) before death. The relative
599 abundance was expressed as RPKM (reads per kilobase of transcript, per million mapped
600 reads).

601

602 **Figure 3 Occurrence of *plcP-agt* genes in major *Pseudomonas* groups.** The
603 phylogeny of *Pseudomonas* clades was determined using the nucleotide sequences of six
604 housekeeping genes (*rpoB, rpoD, dnaE, recA, atpD, gyrB*) retrieved from each genome
605 using IQ-Tree (40). The filled colour indicates the presence of the genes in the genomes
606 whereas a blank indicates the absence of the corresponding gene in the genomes. The
607 two-component system PhoBR (black circles) is found in all genomes and the PlcP-
608 Agt1/Agt2 are strictly conserved in all 770 genome-sequenced *P. aeruginosa* strains that
609 form three clades represented by strain PA14, PA01 and PA7 respectively.

610

611 **Figure 4**, **Characterization of glycolipid formation from recombinant Agt1 and** A**gt2.**
612 **a)** Extracted ion chromatogram of the MGDG lipid from recombinant *E. coli* expressing
613 Agt1. An empty vector control is also shown (red line). The identity of MGDG is further
614 validated using mass spectrometry fragmentation showing the neutral loss of 179
615 corresponding to the loss of glucose and the formation of monoacylglycerols (MAG) with
616 C16:0 or C18:1 (*m/z* 313, 339).

617 **b)** Extracted ion chromatogram of the GADG lipid from recombinant *E. coli* expressing
618 Agt2. An empty vector control is also shown (red line). The identity of GADG is further
619 validated using mass spectrometry fragmentation showing the neutral loss of 193
620 corresponding to the loss of glucose and the formation of monoacylglycerols (MAG) with
621 C16:0 or C18:1 (*m/z* 313, 339).

622 **c)** Purified Agt1 and Agt2 protein from recombinant *E. coli* (left panel) and Michaelis
623 Menten kinetics of Agt1 towards UDP-glucose (middle panel) and Agt2 towards UDP-
624 glucuronic acid (right panel) as substrate, respectively.

625 **d)** Mass spectrometry identification of MGDG and MADG produced from purified Agt1 and
626 Agt2 using DAG and UDP-glucose and UDP-glucuronic acid as the substrate,
627 respectively.

628

629 **Figure 5 Glycolipid formation in *P. aeruginosa* and mutants under Pi stress,**
630 **showing a protective role of glycolipids to polymyxinB.**

631 **a-b)** Relative abundance of the glycolipid MGDG (**a**) and GADG (**b**) in *P. aeruginosa*
632 mutants *plcP* (purple trace), *agt1* (blue trace) and *agt2* (green, trace) compared to the wild
633 type (WT). Cells were cultivated under low phosphate conditions (50 μM) and a
634 representative extracted ion chromatogram of MGDG/GADG is show between the WT,
635 (black trace) and each mutant. The right most panel shows the abundance of MGDG or
636 GADG calculated relative to an internal lipid standard d17:1/12:0
637 sphingosylphosphoethanolamine (Sigma-Aldrich) in the wild-type and mutant strains of *P.*
638 *aeruginosa*. Values are calculated from three biological replicates and the error bars
639 denote standard deviation. MGDG, monoglycosyldiacylglycerol, GADG, glucuronic acid-
640 diacylglycerol.

641 **c)** Survival of glycolipid remodelling mutants Δ*plcP* (purple), Δ*agt1* (green) and Δ*agt2*
642 (blue) when challenged with 4 μg mL^{-1} polymyxin B compared to WT under P stress
643 (black). All experiments were conducted under Pi stress conditions and the results are the
644 average of three biological replicates; error bars denote standard deviation.

645 **d)** Survival of glycolipid producing *Escherichia coli* when challenged with 20 μg mL^{-1}
646 polymyxin B. All experiments were conducted in three replicates and error bars denote
647 standard deviation. Black, *E. coli* containing the empty vector pET28a; green, *E. coli*
648 containing plasmid pET28a-Agt1; blue, *E. coli* containing plasmid pET28a-Agt2.

649

650 **Supplementary Tables**

651

652 **Suppl. Table S1** Proteomic analysis of differentially expressed proteins in the wild-type
653 *P. aeruginosa* PAO1 in response to different phosphate levels (1 mM versus 50 μM).

654

655 **Suppl. Table S2** Protein BLAST identification of locus tags homologous to *agt1* and *agt2*
656 glycolipid synthesis genes in all genome sequenced *P. aeruginosa* strains at the JGI IMG
657 database.

658

659 **Suppl. Table S3** Proteomic analysis of wild type *P. aeruginosa* PAO1 versus the Δ*plcP*
660 mutant grown at 50 μM phosphate.

661

662 **Suppl. Table S4** Whole genome mapping to *Pseudomonas aeruginosa* PAO1 of a
663 metatranscriptomic dataset (SRX5145605, SRX5145606) from sputum samples taken
664 from a cystic fibrosis patient 7 and 8 days before death. **S4A** (SRX5145605)**, S4B**
665 (SRX5145606)**.** RPKM, reads per kilobase of transcript per million mapped reads; FPKM,
666 fragments per kilobase of transcript per million mapped reads.

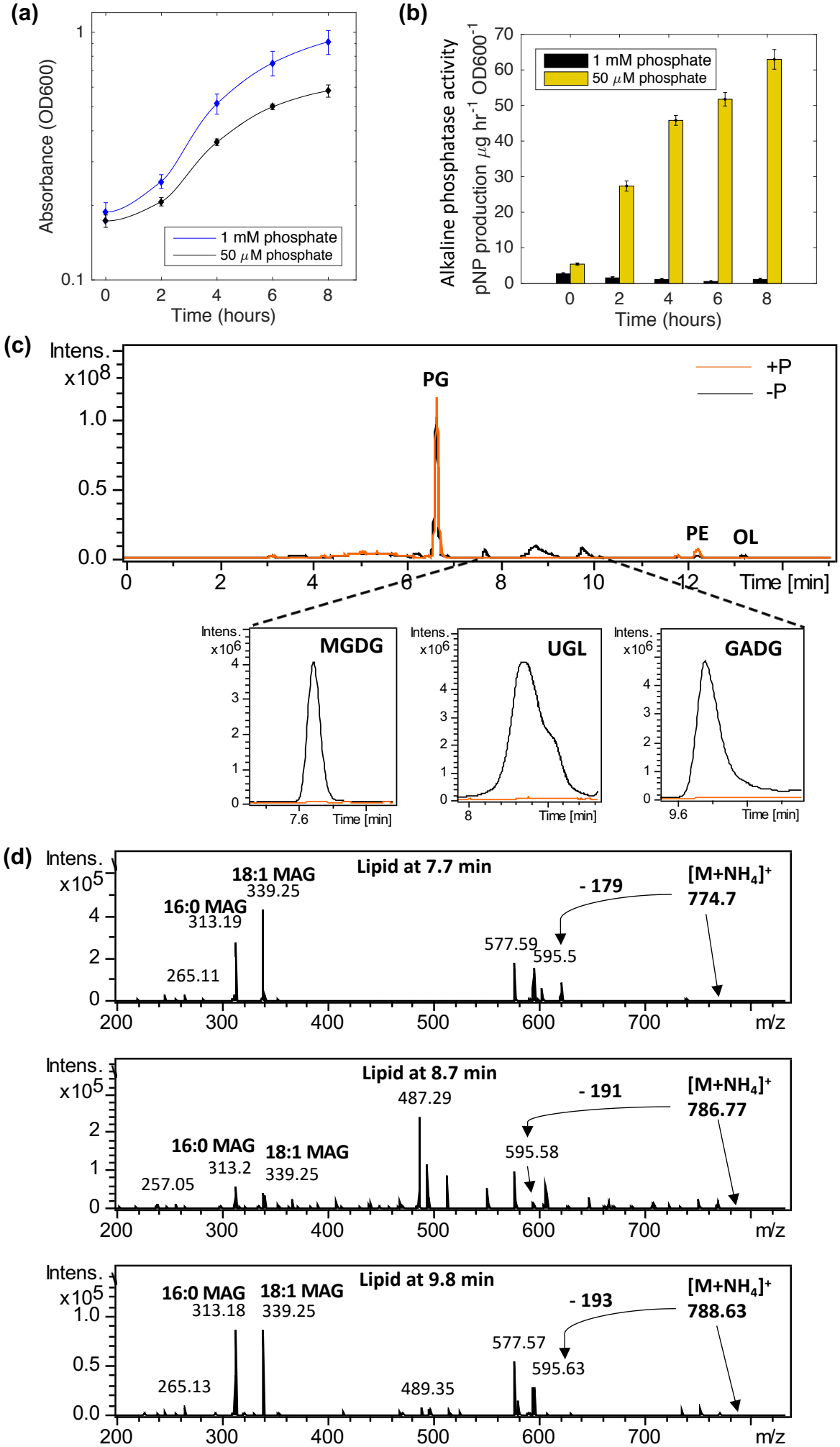
(a)
Absorbance (OD600)
Time (hours)
1 mM phosphate
50 μM phosphate
(b)
Alkaline phosphatase activity
pNP production μg hr-1 OD600-1
Time (hours)
1 mM phosphate
50 μM phosphate
(c)
Intens.
x10^8
PG
+P
-P
PE
OL
Time [min]
MGDG
UGL
GADG
Intens.
x10^6
Time [min]
(d)
Lipid at 7.7 min
18:1 MAG
339.25
16:0 MAG
313.19
265.11
577.59
595.5
- 179
[M+NH4]+
774.7
Lipid at 8.7 min
487.29
- 191
[M+NH4]+
786.77
16:0 MAG
313.2
18:1 MAG
339.25
257.05
595.58
Lipid at 9.8 min
16:0 MAG
313.18
18:1 MAG
339.25
265.13
489.35
577.57
595.63
- 193
[M+NH4]+
788.63
Intens.
x10^5
m/z

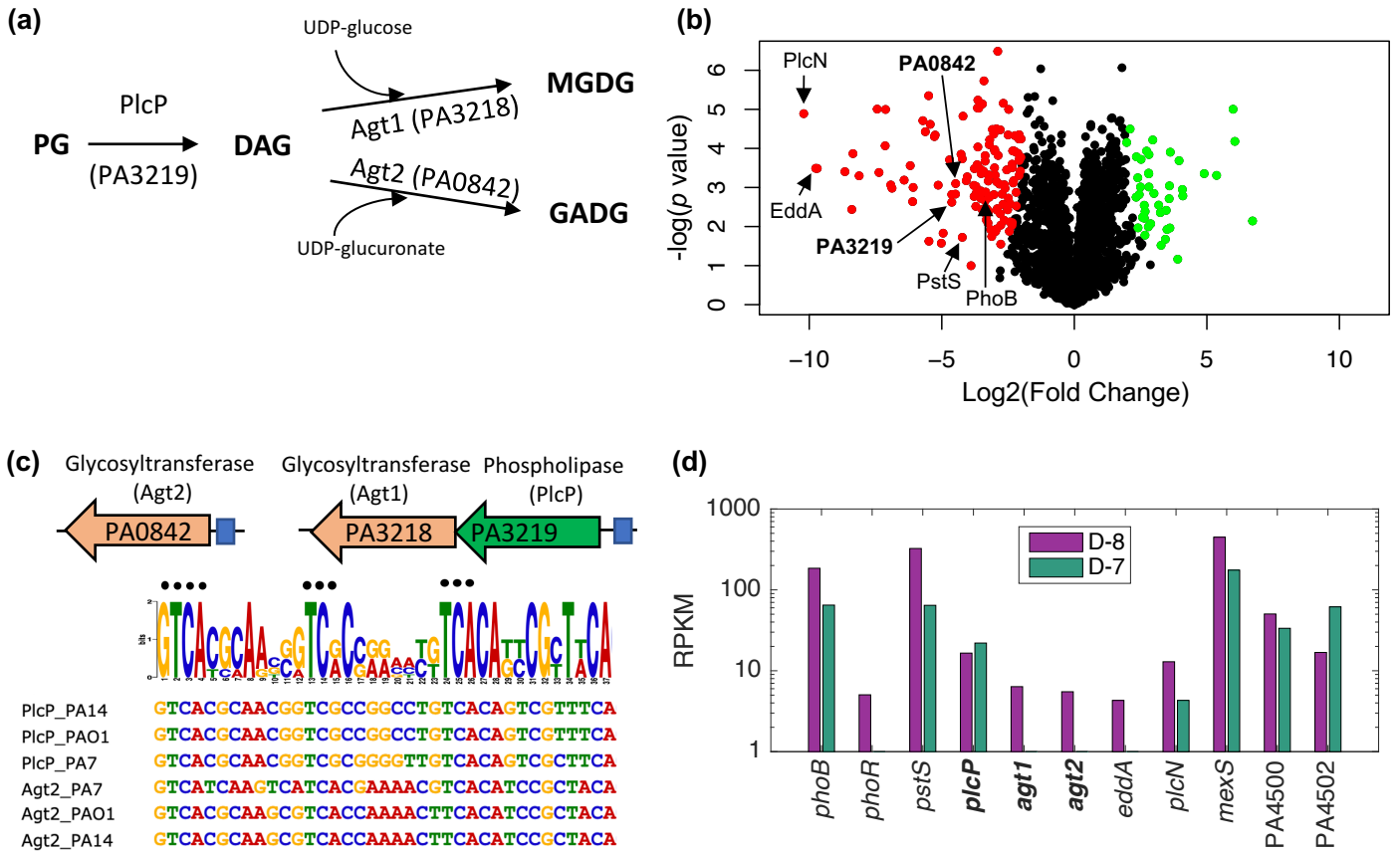
(a)
UDP-glucose
PlcP
PG
(PA3219)
DAG
Agt1 (PA3218)
MGDG
Agt2 (PA0842)
GADG
UDP-glucuronate
(b)
PlcN
PA0842
EddA
PA3219
PstS
PhoB
-log(p value)
Log2(Fold Change)
(c)
Glycosyltransferase (Agt2)
Glycosyltransferase (Agt1)
Phospholipase (PlcP)
PA0842
PA3218
PA3219
PlcP_PA14 GTCACGCAACGGTCGCCGGCCTGTCACAGTCGTTTCA
PlcP_PAO1 GTCACGCAACGGTCGCCGGCCTGTCACAGTCGTTTCA
PlcP_PA7 GTCACGCAACGGTCGCGGGGTTGTCACAGTCGCTTCA
Agt2_PA7 GTCATCAAGTCATCACGAAAACGTCACATCCGCTACA
Agt2_PAO1 GTCACGCAAGCGTCACCAAAACTTCACATCCGCTACA
Agt2_PA14 GTCACGCAAGCGTCACCAAAACTTCACATCCGCTACA
(d)
RPKM
D-8
D-7
phoB
phoR
pstS
plcP
agt1
agt2
eddA
plcN
mexS
PA4500
PA4502

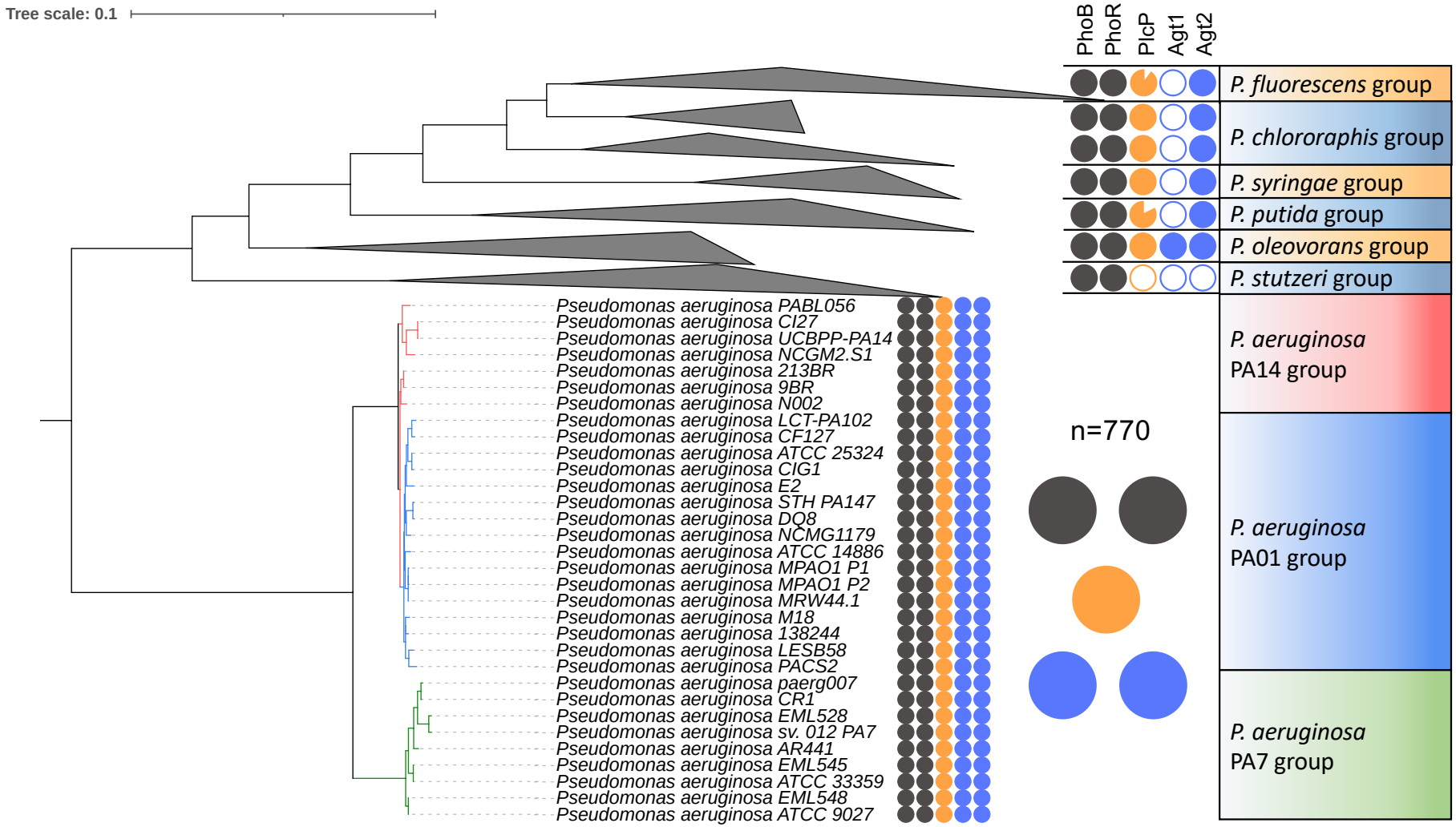
Tree scale: 0.1
PhoB
PhoR
PlcP
Agt1
Agt2
P. fluorescens group
P. chlororaphis group
P. syringae group
P. putida group
P. oleovorans group
P. stutzeri group
P. aeruginosa PA14 group
P. aeruginosa PA01 group
P. aeruginosa PA7 group
n=770
Pseudomonas aeruginosa PABL056
Pseudomonas aeruginosa CI27
Pseudomonas aeruginosa UCBPP-PA14
Pseudomonas aeruginosa NCGM2.S1
Pseudomonas aeruginosa 213BR
Pseudomonas aeruginosa 9BR
Pseudomonas aeruginosa N002
Pseudomonas aeruginosa LCT-PA102
Pseudomonas aeruginosa CF127
Pseudomonas aeruginosa ATCC 25324
Pseudomonas aeruginosa CIG1
Pseudomonas aeruginosa E2
Pseudomonas aeruginosa STH PA147
Pseudomonas aeruginosa DQ8
Pseudomonas aeruginosa NCMG1179
Pseudomonas aeruginosa ATCC 14886
Pseudomonas aeruginosa MPAO1 P1
Pseudomonas aeruginosa MPAO1 P2
Pseudomonas aeruginosa MRW44.1
Pseudomonas aeruginosa M18
Pseudomonas aeruginosa 138244
Pseudomonas aeruginosa LESB58
Pseudomonas aeruginosa PACS2
Pseudomonas aeruginosa paerg007
Pseudomonas aeruginosa CR1
Pseudomonas aeruginosa EML528
Pseudomonas aeruginosa sv. 012 PA7
Pseudomonas aeruginosa AR441
Pseudomonas aeruginosa EML545
Pseudomonas aeruginosa ATCC 33359
Pseudomonas aeruginosa EML548
Pseudomonas aeruginosa ATCC 9027

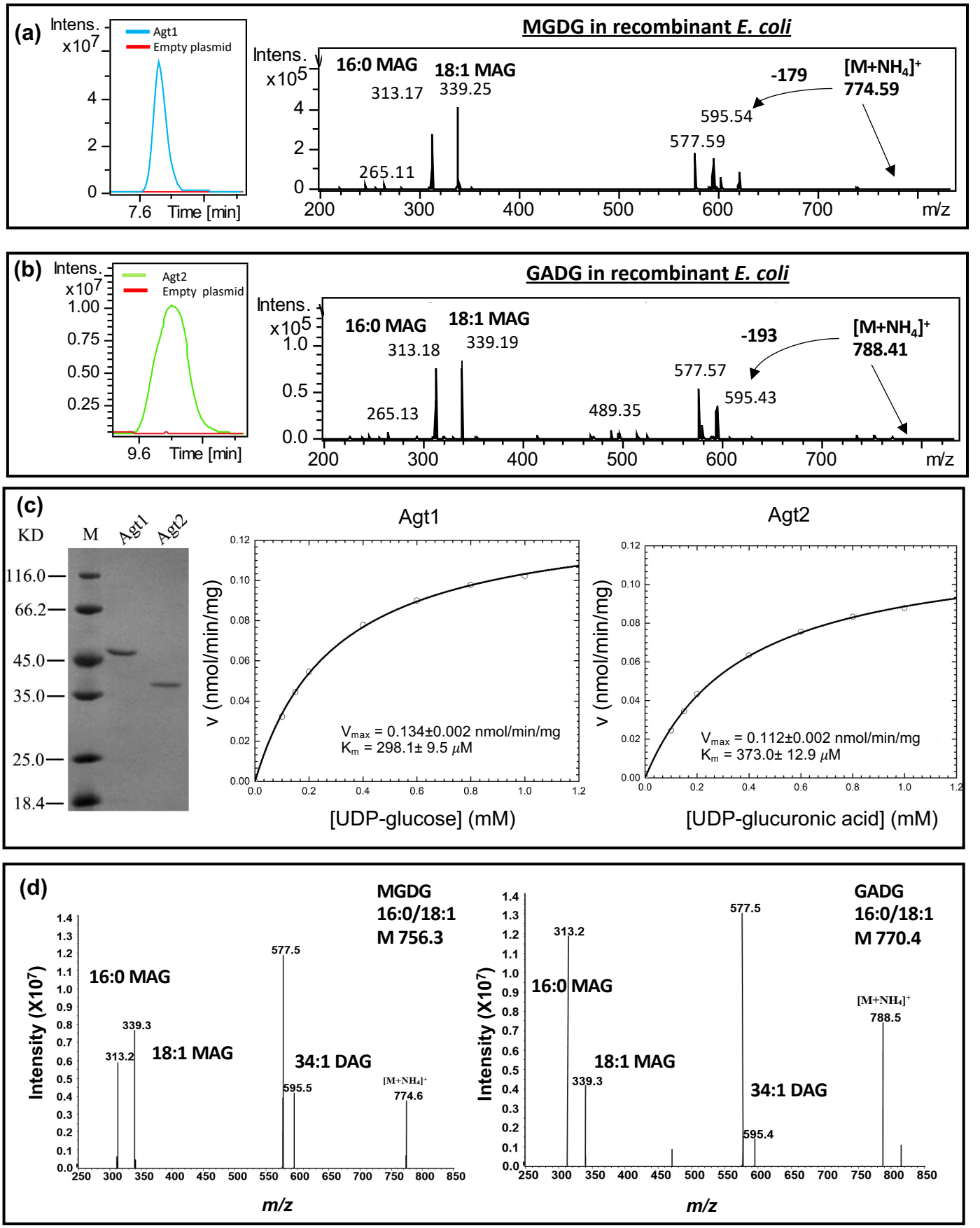
(a)
MGDG in recombinant E. coli
Intens.
x10^7
Agt1
Empty plasmid
7.6 Time [min]
Intens.
x10^5
16:0 MAG
18:1 MAG
313.17
339.25
265.11
577.59
595.54
-179
[M+NH4]+
774.59
m/z
(b)
GADG in recombinant E. coli
Intens.
x10^7
Agt2
Empty plasmid
9.6 Time [min]
Intens.
x10^5
16:0 MAG
18:1 MAG
313.18
339.19
265.13
489.35
577.57
595.43
-193
[M+NH4]+
788.41
m/z
(c)
KD
M
Agt1
Agt2
116.0
66.2
45.0
35.0
25.0
18.4
Agt1
v (nmol/min/mg)
Vmax = 0.134±0.002 nmol/min/mg
Km = 298.1± 9.5 μM
[UDP-glucose] (mM)
Agt2
v (nmol/min/mg)
Vmax = 0.112±0.002 nmol/min/mg
Km = 373.0± 12.9 μM
[UDP-glucuronic acid] (mM)
(d)
MGDG
16:0/18:1
M 756.3
Intensity (X10^7)
16:0 MAG
18:1 MAG
34:1 DAG
313.2
339.3
577.5
595.5
[M+NH4]+
774.6
m/z
GADG
16:0/18:1
M 770.4
Intensity (X10^7)
16:0 MAG
18:1 MAG
34:1 DAG
313.2
339.3
577.5
595.4
[M+NH4]+
788.5
m/z

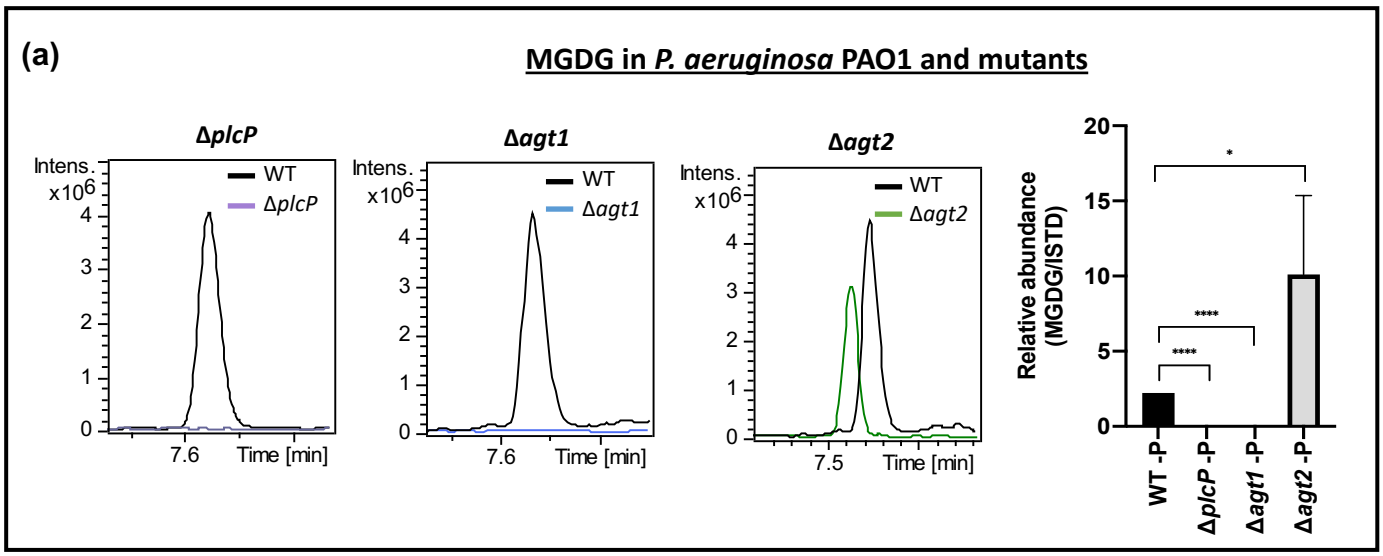
(a)
MGDG in P. aeruginosa PAO1 and mutants
ΔplcP
Δagt1
Δagt2
Intens.
x10^6
WT
ΔplcP
Δagt1
Δagt2
7.6
7.5
Time [min]
Relative abundance (MGDG/ISTD)
WT -P
ΔplcP -P
Δagt1 -P
Δagt2 -P

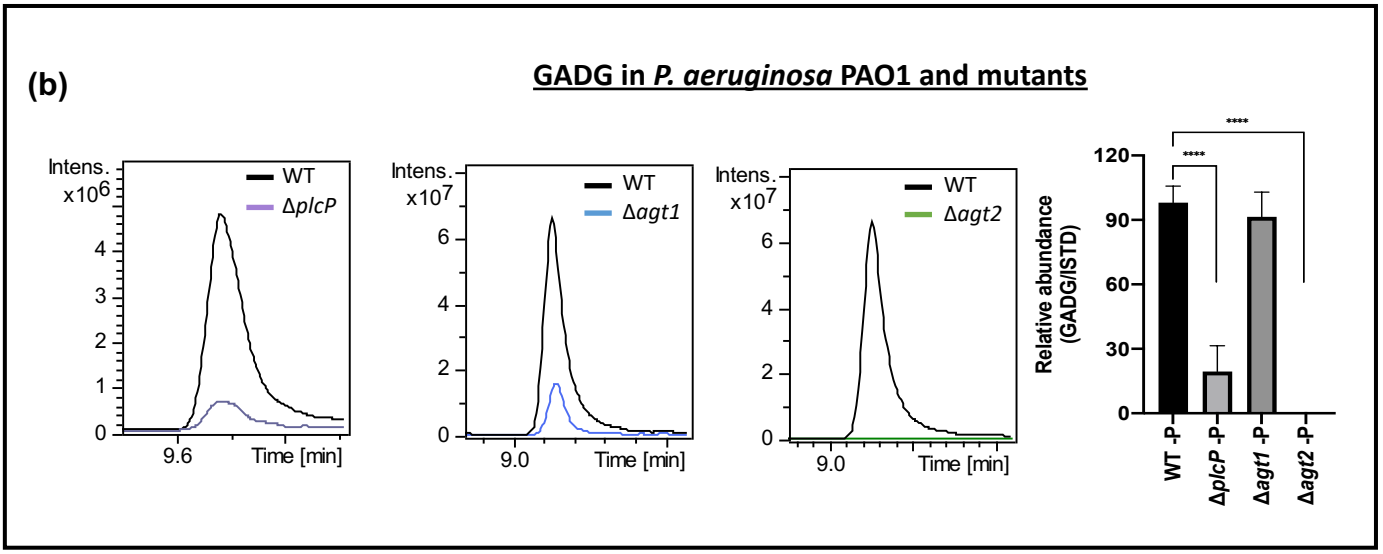
(b)
GADG in P. aeruginosa PAO1 and mutants
Intens.
x10^6
x10^7
WT
ΔplcP
Δagt1
Δagt2
9.6
9.0
Time [min]
Relative abundance (GADG/ISTD)
WT -P
ΔplcP -P
Δagt1 -P
Δagt2 -P

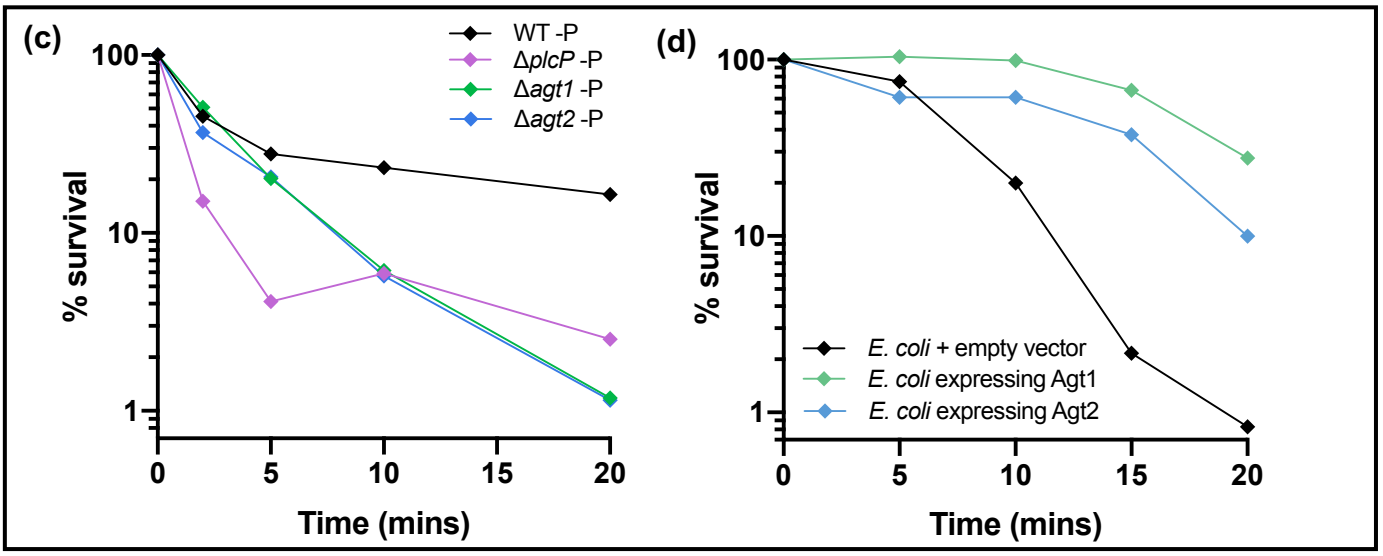
(c)
WT -P
ΔplcP -P
Δagt1 -P
Δagt2 -P
% survival
Time (mins)
(d)
E. coli + empty vector
E. coli expressing Agt1
E. coli expressing Agt2
% survival
Time (mins)